J. Phys.: Condens. Matter **11** (1999) 8283–8289. Printed in the UK PII: S0953-8984(99)03728-5

Nuclear quadrupole interactions of ^{11}B in β-BaB_2O_4 single crystal studied by nuclear magnetic resonance

In Gyoo Kim and Sung Ho Choh

Department of Physics, Korea University, Seoul 136-701, Korea

Received 26 April 1999, in final form 19 July 1999

Abstract. For the low-temperature phase β-BaB_2O_4 single crystal, the rotation patterns of the nuclear magnetic resonance spectra of the ^{11}B nucleus were measured in the three mutually perpendicular crystal planes. We observed twelve sets of different spectra which can be divided into two groups. The six sets in each group have the same principal values of the electric field gradient tensor and originate from the chemically equivalent but magnetically inequivalent sites. The nuclear quadrupole coupling constant (e^2qQ/h) and the asymmetry parameter (η) at room temperature were determined in this study for the first time, and are as follows: for B(1), $e^2qQ/h = 2.455 \pm 0.006$ MHz and $\eta = 0.684 \pm 0.015$; and for B(2), $e^2qQ/h = 2.486 \pm 0.006$ MHz and $\eta = 0.644 \pm 0.019$. The principal-axis orientations of the electric field gradient tensors were also determined. By investigating the temperature dependence of the quadrupole splittings, we find that the basic structural unit of the crystal hardly changes with temperature in the range 140–420 K.

1. Introduction

The β-BaB_2O_4 (barium metaborate, BBO) crystal has attracted a great deal of attention as a frequency doubler, like LiB_3O_5 and $KTiOPO_4$, because of its highly non-linear optical (NLO) properties [1–6]. It has a wide range of transparency in both the ultraviolet and the near-infrared and has large birefringence which allows the generation of even the fifth harmonics of a Nd:YAG laser [4]. The optical, mechanical, and thermal properties [7], the defects [8], and the vibrational modes [9] have been reported.

There are two known phases for BBO [10]; one is the quenched high-temperature form (α-BaB_2O_4) of space group $R3c$ (C_{3v}^6) [11], and the other is the low-temperature phase (β-BaB_2O_4) of the same space group as α-BaB_2O_4 [12–14]. Since α-BaB_2O_4 is centro-symmetric, it does not show NLO properties [15]. The crystal structure of the low-temperature phase is trigonal, and the lattice constants are $a = 12.532$ Å and $c = 12.717$ Å at room temperature. There are two $Ba_3(B_3O_6)_2$ molecules in a primitive unit cell. It consists of nearly planar anionic $(B_3O_6)^{3-}$ ring groups with D_{3h} symmetry, and the anion plane is perpendicular to the threefold axis. There are two kinds of boron atom (B(1) and B(2)) which form different boron–oxygen rings, and, therefore, lie at chemically inequivalent sites. These anionic groups are bonded ionically through barium ions. There are four anionic groups in each primitive unit cell, which are distributed over two symmetrically independent positions.

In this work, we studied the local structure around the boron atoms by investigating the quadrupole interactions of the ^{11}B nucleus. The angular dependences of the ^{11}B nuclear magnetic resonance (NMR) spectra were measured for the low-temperature phase of barium metaborate at 4.7 T. The quadrupole Hamiltonian parameters, i.e., the nuclear quadrupole

0953-8984/99/428283+07$30.00

coupling constant (e^2qQ/h) and the asymmetry parameter (η), are evaluated, and the principal axes of the electric field gradient (EFG) tensor are also determined.

2. Experiments

The BBO single crystal, grown by the modified flux method at CASIX in China, was cut along two crystallographic axes (the *a*-, *c*-axes), and another axis (the *b*-axis) perpendicular to these axes. After the crystal axes were identified by employing an x-ray diffractometer, the sample was mounted perpendicular to one of the crystal faces (*ab*-, *bc*-, and *ca*-planes). It was inserted into the goniometer probe which was capable of rotating the sample with a precision of 1/60 of a degree. The rotation patterns were measured at room temperature by employing a Bruker MSL 200S pulsed NMR spectrometer. The static magnetic field of 4.7 T was applied by a superconducting magnet. A single pulse having the width 1 μs was used. The repetition time and the ring-down delay time were about ten minutes and 6 μs, respectively. The carrier frequency of the pulse was varied in the range $\omega_0/2\pi = 63.2$–65.2 MHz in order to excite all of the satellite lines of the ^{11}B NMR. In the magnetic field used in the experiment, the Larmor frequency of the ^{11}B nucleus was 64.2 MHz. The temperature dependence of the resonance frequencies was measured in several magnetic field directions over the range 140–420 K.

3. Results and discussion

^{11}B is a quadrupolar nucleus with a nuclear spin (I) of 3/2. When this nucleus is located in a non-zero electric field gradient (EFG), it gives $2I$ resonance lines for the case in which the nuclear quadrupole interaction perturbs the Zeeman energy levels. One of them is the central transition line ($|1/2\rangle \leftrightarrow |-1/2\rangle$) and two others are satellite ones ($|3/2\rangle \leftrightarrow |1/2\rangle$ and $|-3/2\rangle \leftrightarrow |-1/2\rangle$). Therefore, if the local symmetry around the boron atoms is not cubic, a boron atom gives three resonance lines, and 12 boron atoms in a BBO unit cell give a total of 24 satellite lines. The 24 satellite lines become degenerate and reduce to 12 lines when the applied magnetic field is parallel to one of the crystallographic axes, as shown in figure 1. In this figure, the splitting of the central line is caused by the second-order perturbation of the nuclear Zeeman interaction by the quadrupole interaction.

After inspecting the rotation patterns of the NMR spectra in three mutually perpendicular planes (figure 2), we divided the spectra into two groups with six sets in each group, called B(1) and B(2). In the *ab*-plane, there is a 60° period in the rotation patterns. This periodicity is caused by the threefold rotational symmetry around the *c*-axis, and this fact implies that the boron atoms do not lie on the threefold axis. In the *bc*- and *ca*-planes, the resonance frequencies reach their maximum values near the *c*-axis, which means that the direction of the principal Z-axis of the EFG tensor is almost the same as the *c*-axis direction.

The NMR spectra of the ^{11}B nucleus for each group were analysed using the usual Hamiltonian [16]:

$$H = H_Z + H_Q \tag{1}$$

where H_Z is the nuclear Zeeman interaction and H_Q the nuclear electric quadrupole interaction. In the principal-axis system of the EFG tensor, H_Q becomes

$$H_Q = \frac{e^2qQ}{4I(2I-1)}\left\{3I_Z^2 - I^2 + \frac{1}{2}\eta(I_+^2 + I_-^2)\right\} \tag{2}$$

where e^2qQ/h is the nuclear quadrupole coupling constant. Again, H_Q is expressed as

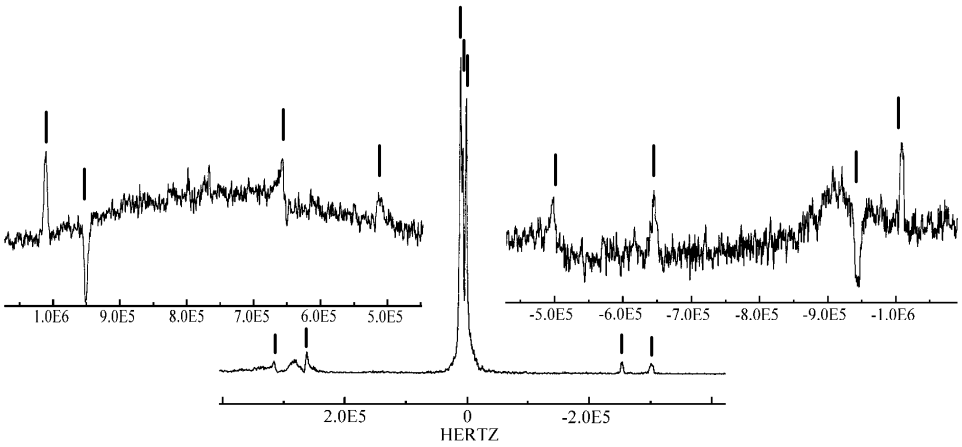

Figure 1. Typical NMR spectra of ^{11}B in a β-BaB_2O_4 single crystal at room temperature, when the magnetic field is applied along the *b*-axis. The frequency 0 corresponds to the Larmor frequency 64.2 MHz of the ^{11}B nucleus at 4.7 T. Since a single pulse was not able to excite all of the NMR signals, the signal acquisitions were performed at three different carrier frequencies, i.e., 65.0, 64.2, and 63.4 MHz.

follows [17]:

$$H_Q = \hat{I}^{\mathrm{t}} \tilde{P} \hat{I} \tag{3}$$

by introducing the nuclear spin operator $\hat{I}$ and the nuclear quadrupole coupling matrix $\tilde{P}$. The $\tilde{P}$ matrix is symmetric and traceless:

$$\tilde{P} = P \begin{pmatrix} \eta - 1 & 0 & 0 \\ 0 & -\eta - 1 & 0 \\ 0 & 0 & 2 \end{pmatrix} \tag{4}$$

where

$$P = \frac{e^2 q Q}{4I(2I-1)}. \tag{5}$$

Since the nuclear spin of ^{11}B is 3/2, $P = e^2 q Q/12$. By using the EPR–NMR program which adopts the diagonalization algorithm of the matrix representation of the Hamiltonian [18] instead of the perturbation method of Volkoff [19], we determined the principal values and the principal directions of the EFG tensor.

The final best fit of the quadrupole parameters of ^{11}B in the β-BaB_2O_4 crystal is given in table 1. The best-fit values for the B(1) and B(2) atoms are very similar. We assigned values to each atom by considering two aspects. First, as explained above, the β-BaB_2O_4 crystal consists of planar $(B_3O_6)^{3-}$ rings. The nearest-neighbour B(1)–O bond lengths are 1.329,

Table 1. The nuclear quadrupole coupling constant and the asymmetry parameter of $^{11}B(1)$ and $^{11}B(2)$ in the β-BaB_2O_4 crystal near 300 K.

	B(1)	B(2)
e^2qQ/h (MHz)	2.455 ± 0.006	2.486 ± 0.006
η	0.684 ± 0.015	0.644 ± 0.019

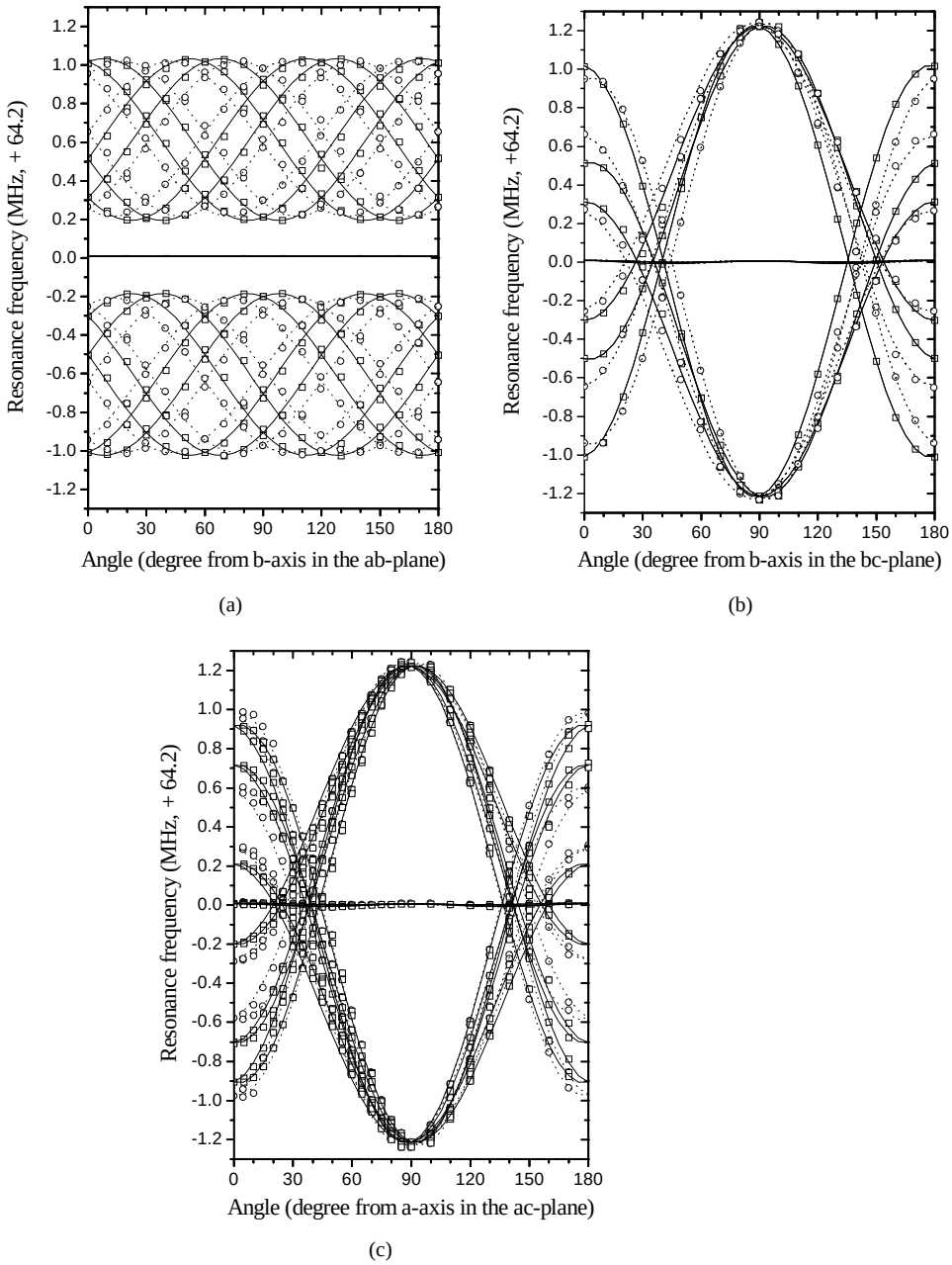

Figure 2. The rotation patterns of ^{11}B NMR spectra in the BBO crystal in the (a) *ab*-plane, (b) *bc*-plane, and (c) *ca*-plane. The experimental data for B(1) and B(2) are plotted as open squares and circles, respectively. The solid and dotted lines show the resonance frequencies calculated with the parameters given in table 1.

1.415, and 1.396 Å, and the average distance is 1.377 Å, while the B(2)–O bond lengths are 1.336, 1.398, and 1.378 Å and the average distance is 1.371 Å. The bond angles are 117.9°, 117.7°, and 124.6° for B(1), and 122.0°, 121.0°, 118.0° for B(2) [7]. The B(2)–O triangle has

rather shorter bond lengths and more symmetric bond angles than the B(1)–O triangle. Since the electric field gradient is proportional to $1/r^3$ and the asymmetry parameter represents the anisotropy of the EFG tensor, the B(1) site is expected to have a smaller e^2qQ/h and a larger η than the B(2) site. Second, if an ^{11}B nucleus lay in the centre of the boron–oxygen regular triangle, then the principal Z-axis of the EFG tensor would coincide with the normal to the plane. One of the EFG tensors, corresponding to one set in each group, and its principal directions are shown in table 2. The remaining five tensors for each group can be obtained by similarity transformations which rely on the symmetry relations of the crystal:

$$\tilde{P}_i = \tilde{R}_i \tilde{P} \tilde{R}_i^{\mathrm{t}} \tag{6}$$

where $\tilde{R}_i$ is a symmetry operation, such as 120° and 240° rotation around the c-axis, or reflection in the mirror planes perpendicular to the [100], [010], and $[\bar{1}\bar{1}0]$ directions. The $\tilde{R}_i$s are calculated as follows:

$$\tilde{R}_{2\pi/3} = \begin{pmatrix} \cos(2\pi/3) & \sin(2\pi/3) & 0 \\ -\sin(2\pi/3) & \cos(2\pi/3) & 0 \\ 0 & 0 & 1 \end{pmatrix} \qquad \tilde{R}_{4\pi/3} = \begin{pmatrix} \cos(4\pi/3) & \sin(4\pi/3) & 0 \\ -\sin(4\pi/3) & \cos(4\pi/3) & 0 \\ 0 & 0 & 1 \end{pmatrix}$$

$$\tilde{R}_{\perp[100]} = \begin{pmatrix} -1 & 0 & 0 \\ 0 & 1 & 0 \\ 0 & 0 & 1 \end{pmatrix} \qquad \tilde{R}_{\perp[010]} = \begin{pmatrix} 1/2 & \sqrt{3}/2 & 0 \\ \sqrt{3}/2 & -1/2 & 0 \\ 0 & 0 & 1 \end{pmatrix} \tag{7}$$

$$\tilde{R}_{\perp[\bar{1}\bar{1}0]} = \begin{pmatrix} 1/2 & -\sqrt{3}/2 & 0 \\ -\sqrt{3}/2 & -1/2 & 0 \\ 0 & 0 & 1 \end{pmatrix}.$$

Using the values in table 2, we display the principal axes with respect to the boron–oxygen bond directions in figure 3. The Z-axis orients nearly perpendicularly to the boron–oxygen triangle and the X-axis is approximately along one of the B–O bonds.

Table 2. The EFG tensor in MHz and its principal directions in polar coordinates (θ, ϕ) for B(1) and B(2) sites.

	B(1)	B(2)
EFG tensor	$\begin{pmatrix} -0.06747 & -0.02948 & 0.02185 \\ -0.02948 & -0.33859 & 0.02797 \\ 0.02185 & 0.02797 & 0.40606 \end{pmatrix}$	$\begin{pmatrix} -0.32584 & -0.06490 & 0.05084 \\ -0.06490 & -0.08859 & 0.00208 \\ 0.05084 & 0.00208 & 0.41443 \end{pmatrix}$
Principal directions	(87.7°, 173.6°)	(88.8°, 104.1°)
	(87.7°, 263.7°)	(86.3°, 194.2°)
X, Y, Z	(3.2°, 39.3°)	(3.9°, 356.1°)

The quadrupole splitting was measured in the temperature range 140–400 K and found to be nearly constant. Therefore, the local symmetry around the boron atoms is hardly modified by the temperature change investigated. According to reports on the temperature dependence of the lattice constants of the β-BaB_2O_4 crystal [20,21], the thermal expansion coefficients for the a- and c-axis and the volume coefficient at 300 K are $7.601 \times 10^{-6}\,\mathrm{K}^{-1}$, $3.356 \times 10^{-5}\,\mathrm{K}^{-1}$, and $3.531 \times 10^{-5}\,\mathrm{K}^{-1}$, respectively. From 140 K to 400 K, the lattice constant and the volume increase by less than 1%. However, the local structure around the boron atoms hardly changes according to the NMR results over the temperature range investigated.

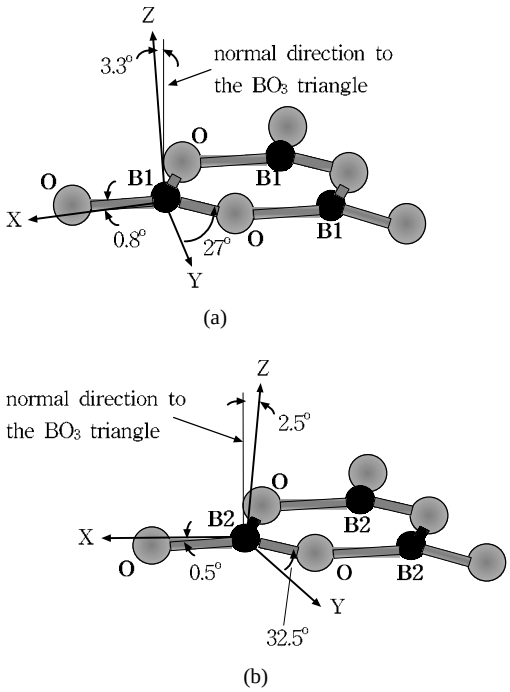

Figure 3. The relationship between the principal axes of the EFG tensor and the boron–oxygen bonds are shown in (a) for B(1) and (b) for B(2), in terms of the angles between the principal axes (the Z-, X-, and Y-axes) and the BO_3 plane normal, the outer boron–oxygen bond of the ring, and another boron–oxygen bond, respectively. The threefold axis (the c-axis) runs approximately perpendicularly to the $(B_3O_6)^{3-}$ rings.

There is an interesting aspect of the parameters of the quadrupole Hamiltonian and the non-linear optical property. Inspecting the parameters of our previous results [22], there seem to be close relations between the parameters of the quadrupole Hamiltonian and the effective non-linear optical coefficients (d_{eff}) for the second-harmonic generation (SHG) [23]. For the single crystals of $Li_2B_4O_7$, LiB_3O_5, and KB5, together with BBO, a crystal which has a larger asymmetry parameter for ^{11}B among the threefold-coordinated boron atoms has a larger d_{eff}. The BBO crystal has the largest asymmetry parameters for ^{11}B among the threefold-coordinated boron atoms of the above crystals and has the largest d_{eff} for SHG.

4. Conclusions

The nuclear quadrupole coupling constant and the asymmetry parameter of the ^{11}B nucleus in β-BaB_2O_4 are determined here for the first time; they are summarized in table 1. For B(1) and B(2) atoms, the principal Z-axis of the EFG tensor is nearly parallel to the crystallographic c-axis, and the X-axis is oriented approximately parallel to the outer B–O bond of the $(B_3O_6)^{3-}$ ring. Furthermore, from the temperature dependence study of the quadrupole splitting in the range 140–420 K, we conclude that not only is the macroscopic symmetry of the BBO very stable but so also is the microscopic symmetry, i.e., the basic structural unit of the crystal hardly changes in this temperature range. Therefore, the BBO crystal could be safely used under extreme conditions, e.g. in very hot or very cold atmospheres.

Acknowledgments

This work was supported by the KOSEF through the RCDAMP at Pusan National University (1997–2000). The NMR experiment was performed at Seoul Branch, Korea Basic Science Institute. The authors also acknowledge Dr H Y Yeom (Dankuk University) and Dr I H Choi (Korea University) for their help with the XRD measurements.

References

[1] Chen C, Wu B, You G and Huang Y 1984 *13th Int. Quantum Electronics Conf.* (Washington, DC: OSA) digest of technical papers, paper MCC5
[2] Chen C, Wu B, Jiang A and You G 1985 *Sci. Sin.* B **28** 235
[3] Kato K 1986 *IEEE J. Quantum Electron.* **22** 1013
[4] Miyazaki K, Sakai H and Sato T 1986 *Opt. Lett.* **11** 797
[5] Zhang G, Jin C, Lin F, Chen C and Wu B 1984 *Guangxue Xuebau* **4** 513
[6] Chen C, Wu Y, Jiang A, Wu B, You G, Li R and Lin S 1989 *J. Opt. Soc. Am.* B **6** 616
[7] Eimerl D, Davis L, Velsko S, Graham E K and Zalkin A 1987 *J. Appl. Phys.* **62** 1968
[8] Tan Q, Mao H, Lin S, Chen H, Lu S, Tang D and Ogawa T 1994 *J. Cryst. Growth* **141** 393
[9] Hong S-L and Wu B 1995 *Opt. Eng.* **34** 1738
[10] Levin E M and McMurdie H F 1949 *J. Res. NBS* **42** 131
[11] Mighell A D, Perloff A and Block S 1966 *Acta Crystallogr.* **20** 819
[12] Hubner K H 1969 *Neues Jahrb. Mineral. Monatsh.* 335
[13] Liebertz J and Stahr Z 1983 *Z. Kristallogr.* **165** 91
[14] Fröhlich R 1984 *Z. Kristallogr.* **168** 109
[15] Itoh K, Maruma F and Kuwano Y 1990 *J. Cryst. Growth* **106** 728
[16] Abragam A 1961 *The Principles of Nuclear Magnetism* (Oxford: Oxford University Press) chs VI, VII
[17] Weil J A, Bolton J R and Wertz J E 1994 *Electron Paramagnetic Resonance* (New York: Wiley) ch 5
[18] Mombourquette M J, Weil J A and McGavin D G 1995 *Operation Instructions for Computer Program EPR–NMR version 6.0* Department of Chemistry, University of Saskatchewan
[19] Volkoff G M 1953 *Can. J. Phys.* **31** 361
[20] Oyama Y, Yabashi H, Hasegawa M and Takei H 1994 *Ferroelectrics* **152** 361
[21] Sheleg A U, Zub E M, Stremoukhova L A and Luginets A M 1997 *Phys. Solid State* **39** 932
[22] Kim I G, Choh S H and Kim J N 1998 *J. Korean Phys. Soc.* **32** S669
[23] Kim I G and Choh S H 1999 *Bull. Am. Phys. Soc.* **44** 370